Dielectric Resonator Antennas: From Multifunction Microwave Devices to Optical Nano-antennas

by

Longfang Zou

Bachelor of Engineering,
The University of Electronic Science and Technology of China, China, 1999

Master of Engineering, Southwest Jiaotong University, China, 2005

Master of Engineering, The University of Adelaide, Australia, 2008

Thesis submitted for the degree of

Doctor of Philosophy

in

School of Electrical and Electronic Engineering The University of Adelaide, Australia

March 2013

© 2013 Longfang Zou All Rights Reserved



Contents

Content	nts	iii
Abstrac	ct	vii
Statem	nent of Originality	ix
Acknow	wledgments	хi
Conven	ntions	xiii
Abbrevi	viations	χV
Author	Publications	xvii
List of	Figures	xix
List of	Tables	xxv
Chapter	er 1. Introduction	1
1.1	Introduction and motivation	 2
	1.1.1 Motivation - Multifunction and diversity DRA	 3
	1.1.2 Motivation - Optical DRA	 4
1.2	Objectives of the thesis	 4
1.3	Statement of original contributions	 6
1.4	Overview of the thesis	 9
Chapter	er 2. Rectangular and cylindrical dielectric resonator antenna	13
2.1	Introduction	 14
2.2	Modes of DR	 15
2.3	Rectangular dielectric resonator antenna	 16
	2.3.1 Resonant frequency of the fundamental TE_{111} mode	 17

	2.3.2	Radiation Q-factor of the fundamental TE_{111} mode	20
	2.3.3	Methods for excitation of the fundamental TE_{111} mode	21
2.4	Cyline	drical dielectric resonator antenna	26
	2.4.1	Field distribution, resonant frequency and Q-factor of fundamen-	
		tal modes	27
	2.4.2	$\text{HEM}_{11\delta}$ and $\text{TM}_{01\delta}$ mode excitation methods	29
	2.4.3	$TE_{01\delta}$ mode excitation method	33
2.5	Concl	usion	34
Chapte	r 3. Ci	rcularly polarized dielectric resonator antenna	35
3.1	Introd	luction	36
3.2	Circul	larly polarized DRA configuration	37
	3.2.1	DR design	38
	3.2.2	Feeding network design	41
3.3	Exper	imental results	41
3.4	Radia	tion pattern improvement	45
3.5	Concl	usion	47
Chapte	r 4. M	ultifunction and diversity dielectric resonator antenna	51
4.1	Introd	luction	52
4.2	Multi	function DRA design	53
	4.2.1	Antenna structure	53
	4.2.2	Excitation of the TE_{111} mode from Port 1	54
	4.2.3	Excitation of the Quasi-TM $_{111}$ mode from Port 2	55
	4.2.4	Integrating two ports into a common volume	56
	4.2.5	Feeding network of Port 1 for broadside circular polarization	59
	4.2.6	Impedance bandwidth optimization of Port 2	60
4.3	Anter	nna performance	62
	4.3.1	S parameters	62
	4.3.2	Axial ratio	63
	4.3.3	Radiation patterns and gain	64
	4.3.4	Diversity	67
4.4	Concl	usion	73

Chapte	er 5. Horizontally polarized omnidirectional DRA	75
5.1	Introduction	76
5.2	HP DRA design	78
	5.2.1 Excitation of the $TE_{01\delta}$ mode	78
	5.2.2 Bandwidth enhancement by addition of an air gap	79
	5.2.3 Feeding structure optimization	82
5.3	Fabrication	83
5.4	Experimental results	84
5.5	Conclusion	88
Chapte	er 6. Horizontally and vertically polarized omnidirectional DRA	89
6.1	Introduction	90
6.2	Dual polarized DRA design	91
	6.2.1 DR design	92
	6.2.2 Excitation of $TE_{01\delta}$ Mode	94
	6.2.3 Excitation of the $TM_{01\delta}$ mode	98
6.3	Antenna performance	99
	6.3.1 S parameters	99
	6.3.2 Radiation pattern and gain	100
	6.3.3 Diversity	101
6.4	Conclusion	103
Chapte	er 7. On the scaling of DRAs from microwave towards visible frequencies	105
7.1	Introduction	106
7.2	Approaches for electromagnetic modeling of metal	108
	7.2.1 Classical skin-effect model	108
	7.2.2 Modified relaxation-effect model	108
	7.2.3 Drude model	109
7.3	A scalable DRA model	111
7.4	DRA scaling behaviour	112
7.5	Computational accuracy and expenditure	114
7.6	Excitation of the fundamental mode at optical frequency range	117
7.7	Conclusion	117

Contents

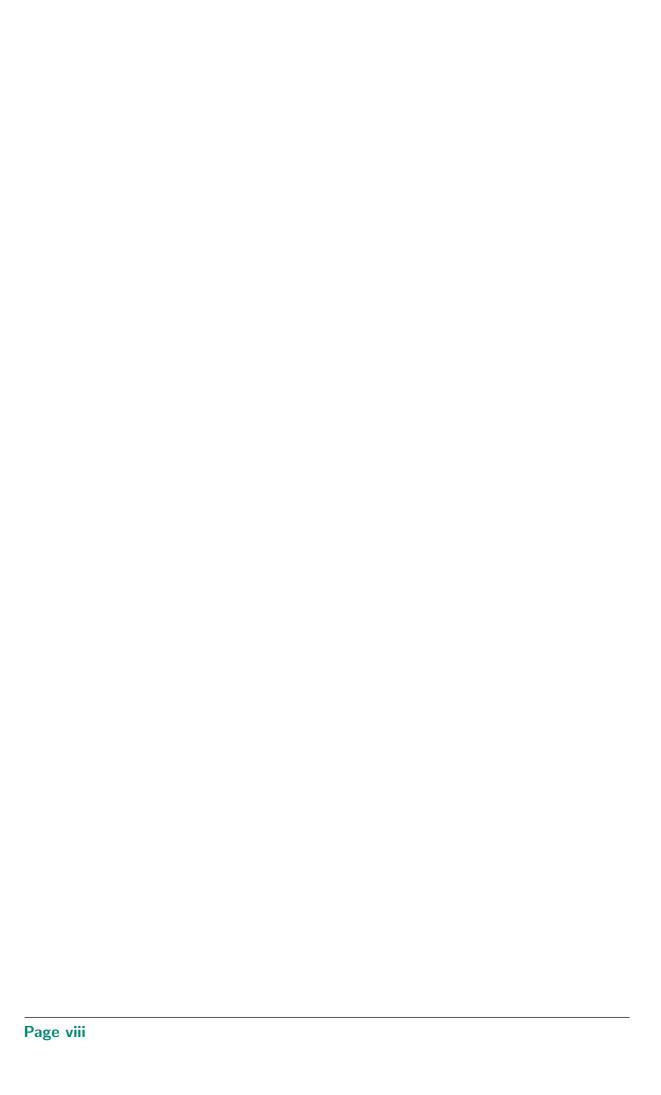
Chapter	8. Op	otical reflectarray of dielectric resonator nano-antennas	121
8.1	Introd	uction	122
8.2	Optica	al DRA reflectarray design	123
	8.2.1	Design principle	124
	8.2.2	TiO ₂ -Silver DR array model	124
	8.2.3	Six-element DRA reflectarray	127
	8.2.4	Four- and nine-element DRA reflectarray	128
8.3	Fabric	ation	130
8.4	First p	rototypes measurement and discussion	132
8.5	Silver	properties measurement	136
8.6	Impro	ved design of optical DRA reflectarray	137
8.7	Second	d prototypes measurement and discussion	138
8.8	Dissip	ation loss in optical DRs	140
	8.8.1	Simulation	141
	8.8.2	Measurement	142
8.9	Comp	arison with grating reflector	144
8.10	Conclu	usion	145
Chapter	9. Co	onclusion and future work	147
9.1	Conclu	usion	148
9.2	Future	ework	152
Bibliogr	aphy		155

Abstract

Since a cylindrical dielectric resonator antenna (DRA) was firstly proposed by Long et al. in the 1980s, extensive research has been carried out on analyzing DRA shapes, characterizing the resonant modes, improving their radiation characteristics with various excitation schemes. Compared with conventional conductor-based antennas, DRAs have attractive features such as small size, high radiation efficiency and versatility in their shape and feeding mechanism.

Importantly, various orthogonal modes with diverse radiation characteristics can be excited within a single DRA element. These modes can be utilized for various requirements, which makes the DRA a suitable potential candidate for multifunction applications. Based on this principle, this thesis presents different multifunction designs: Firstly a cross-shaped DRA with separately fed broadside circularly polarized (CP) and omnidirectional linearly polarized (LP) radiation patterns and, secondly, a multifunction annular cylindrical DRA realizing simultaneously omnidirectional horizontally and vertically polarized radiation patterns with low cross-coupling. The evolution, design process and experimental validation of these two antennas are described in details in the thesis.

The second part of the thesis dramatically scales down DRA to shorter wavelengths. Inspired by the fact that DRA still exhibits high radiation efficiency (>90%) in the millimetre wave range, while the efficiency of conventional metallic antenna degrades rapidly with frequencies, this thesis proposes the concept of nanometer-scale DRA operated in their fundamental mode as optical antennas. To validate the concept, optical DRA reflectarrays have been designed and fabricated. Although the zeroth-order spatial harmonic reflection is observed in the measurement due to the imperfect nanofabrication, the power ratio of deflected beam to the specular component of reflection amounts to 4.42, demonstrating the expected operation of the reflectarray. The results strongly support the concept of optical DRA and proposes design methods and strategies for their realization. This proof of concept is an essential step for future research on nano-DRA as building block of emerging nano-structured optical components.



Statement of Originality

This work contains no material that has been accepted for the award of any other degree or diploma in any university or other tertiary institution and, to the best of my knowledge and belief, contains no material previously published or written by another person, except where due reference has been made in the text.

I give consent to this copy of the thesis, when deposited in the University Library, being available for loan, photocopying, and dissemination through the library digital thesis collection, subject to the provisions of the Copyright Act 1968.

I also give permission for the digital version of my thesis to be made available on the web, via the University's digital research repository, the Library catalogue, the Australasian Digital Thesis Program (ADTP) and also through web search engines, unless permission has been granted by the University to restrict access for a period of time.

Signed	Date	

Acknowledgments

I would like to express my special appreciation and thanks to my principle supervisor, Prof. Christophe Fumeaux, who has been a tremendous mentor for me. I would like to thank him for his thoughtful guidance, constructive suggestions and prompt responses. His advice on both research as well as on my career have been invaluable. I am indebted to my co-supervisor, Dr Withawat Withayachumnankul for his inspiring guidance in the field of metamaterial and nanoantenna and for generously sharing his knowledge and experience. I also wish to express my appreciation to co-supervisor, Prof. Derek Abbott, for his valuable suggestions and constructive advice. My sincere thanks goes to Associate Prof Cheng-Chew Lim for his long term help, encouragement and advice. His professionalism and kindness have been always appreciated.

This thesis would not have been possible without the guidance, cooperation, and assistance of several individuals and research groups. A special mention of thanks to Dr Thomas Kaufmann, Dr Zhonghao Hu, Mr Ali H. Karami, Mr Shifu Zhao, Mr Weixun Wu, Ms Tiaoming Niu, Mr Benjamin S.-Y. Ung, Dr Hungyen Lin and Mr Henry Ho for their fruitful discussions, assistance and critical comments to my research. I am grateful to Mr Pavel Simcik, Mr Brandon Pullen and Mr Ian Linke who fabricated my microwave antenna designs. I express my heart-felt gratitude to Mr Charan Manish Shah, Dr Madhu Bhaskaran, Dr Sharath Sriram, and Prof Arnan Mitchell from the Functional Materials and Microsystems Research Group, RMIT University for fabricating optical dielectric resonator nano-antenna reflectarray and expanding my knowledge of nano-fabrication. Their scientific inputs, personal help and friendly nature have made the cooperation more effective.

I must thank the office & support staff of the School of Electrical and Electronic Engineering, Mr Stephen Guest, Mrs Ivana Rebellato, Ms Rose-Marie Descalzi, Ms Deborah Koch, Ms Jodie Schluter, Mr Danny Di Giacomo, Mr David Bowler, Mr Mark Innes, Mr Ryan King and Mr Anthony Schueller, for their kind support throughout my PhD. They always ready to give their timely help whenever required.

Last but not least, I owe my deepest gratitude to my parents and parents-in-law, for educating me with aspects from arts, engineering and technology, and for unconditional support and encouragement to pursue my interests. I also thank my sisters for giving

Acknowledgments

me moral encouragement all the time. Words are not enough to praise my wife Fang Duan, whose love, support, encouragement and inspiration have guided me through the most challenging times. I must mention my daughter Emily Zou for refreshing my days with her beautiful smile, which has made this long journey possible, endurable, and enjoyable.

Conventions

Typesetting

This thesis is typeset using the LATEX2e software. WinEdt build 5.5 was used as an effective interface to LATEX.

Referencing

Referencing and citation style in this thesis are based on the Institute of Electrical and Electronics Engineers (IEEE) Transaction style.

Units

The units used in this thesis are based on the International System of Units (SI units).

Prefixes

In this thesis, the commonly used numerical prefixes to the SI units are "p" (pico, 10^{-12}), "n" (nano, 10^{-9}), " μ " (micro, 10^{-6}), "m",(milli, 10^{-3}), "k"(kilo, 10^{3}), "M"(mega, 10^{6}), "G"(giga, 10^{9}), and "T"(tera, 10^{12}).

Spelling

The Australian English spelling is adopted in this thesis.



Abbreviations

AR Axial Ratio

BAN Body-Area Network

CP Circularly Polarized

CPW Coplanar Waveguide

DR Dielectric Resonator

DRA Dielectric Resonator Antenna

DWM Dielectric Waveguide Model

EBG Electromagnetic Band Gap

ECC Envelope Correlation Coefficient

EM Electromagnetic

FEM Finite-Element Method

HD High Definition

HEM Hybrid Electric and Magnetic

HFSS High Frequency Structural Simulator (a commercial simulation software)

HMSIW Half-mode Substrate Integrated Waveguide

HP Horizontally Polarized

LHCP Left-Hand Circularly Polarized

LP Linearly Polarized

MEG Mean Effective Gain

MIMO Multiple-Input Multiple-Output

MMW Millimeter Wave

Abbreviations

MNG-TL Mu-Negative Transmission Line

PCB Printed Circuit Board

PEC Perfect Electric Conductor

PIFA Planar Inverted-F Antenna

RHCP Right-Hand Circularly Polarized

SIW Substrate Integrated Waveguide

SPP Surface Plasmon Polariton

TE Transverse Electric

TM Transverse Magnetic

VP Vertically Polarized

WPAN Wireless Personal Area Network

XPR Cross-polarization Power Ratio

Author Publications

Journal

- [1] L. Zou and C. Fumeaux, "A cross-shaped dielectric resonator antenna for multifunction and polarization diversity applications," *IEEE Antennas Wireless Propag. Lett.*, vol. 10, pp. 742-745, Jul. 2011.
- [2] L. Zou, D. Abbott, and C. Fumeaux, "Omnidirectional cylindrical dielectric resonator antenna with dual polarization," *IEEE Antennas Wireless Propag. Lett.*, vol. 11, pp. 515-518, 2012.
- [3] L. Zou, W. Withayachumnankul, C. Shah, A. Mitchell, M. Bhaskaran, S. Sriram, and C. Fumeaux, "Dielectric resonator nanoantennas at visible frequencies," *Opt. Express*, vol. 21, no. 1, pp. 1344-1352, Jan. 2013.

Conference

- [1] L. Zou and C. Fumeaux, "High-permittivity cross-shaped dielectric resonator antenna for circular polarization," in *Int. Conf. Electromagn. Adv. App (ICEAA).*, Sep. 2010, pp. 1-4.
- [2] L. Zou and C. Fumeaux, "Cross-shaped dielectric resonator antenna for circular polarization with symmetric radiation patterns," in *Twelfth Australian Symposium on Antennas*, Feb. 2011.
- [3] L. Zou and C. Fumeaux, "Horizontally polarized omnidirectional dielectric resonator antenna," in *Asia-Pacific Microwave Conference (APMC)*, 2011, Dec. 2011, pp. 849-852.
- [4] L. Zou and C. Fumeaux, "Mutual coupling reduction in a multi-mode multi-function dielectric resonator antenna," in *International Symposium on Antennas and Propagation (APS)*, Jul. 2012. pp. 1-2.

Author Publications

- [5] L. Zou, W. Withayachumnankul, C. Shah, A. Mitchell, M. Bhaskaran, S. Sriram, and C. Fumeaux, "Optical reflectarray based on dielectric resonator antennas," in *Australian Nanotechnology Network (ANN)* 2012 *Early Career Symposium*, Dec. 2012.
- [6] L. Zou, W. Withayachumnankul, C. Shah, A. Mitchell, M. Bhaskaran, S. Sriram, and C. Fumeaux, "Optical dielectric resonator antenna reflectarray," in *Thirteenth Australian Symposium on Antennas*, Feb. 2013.

1.1	The tree diagram of the thesis	10
2.1	Geometry of rectangular DR on a ground plane	17
2.2	Normalized resonant frequency of the TE_{111}^x mode of a rectangular DR	
	(ε_r =10) with different aspect ratio $C = L/b$ and $D = W/b$	20
2.3	Near and far field of TE_{111} mode	22
2.4	Probe coupling to a rectangular DR	22
2.5	Microstrip line coupling to a rectangular DR	23
2.6	Slot aperture coupling to a rectangular DR	24
2.7	Coplanar waveguide coupling to a rectangular DR	24
2.8	SIW structure and field distribution	25
2.9	HMSIW structure and field distribution	26
2.10	SIW fed rectangular DRA	26
2.11	Field distribution of three fundamental modes in a cylindrical DR	27
2.12	Radiation patterns of three fundamental modes of a cylindrical DR	28
2.13	(a) k_0a and (b) Q-factor of the HEM _{11δ} , TM _{01δ} and TE _{01δ} modes of a cylin-	
	drical DR with ε_r =10	29
2.14	Probe coupling to a cylindrical DR	30
2.15	Microstrip line coupling to a cylinder DR	31
2.16	Slot coupling to a cylinder DR	31
2.17	Coplanar waveguide coupling to a cylinder DR	32
2.18	Sketches of the LP and CP HMSIW-fed DRA	32
2.19	A balanced coupling method to excite the $\text{TE}_{01\delta}$ mode in a cylindrical DR	33
3.1	Cross-shaped CP DRA configuration	38
3.2	Calculated DR length and height for a resonance at 4.5 GHz	39
3.3	Simulated DR height and corresponding effective permittivity for a res-	
	onance at 4.5 GHz with different thickness	40

3.4	Simulated E filed distribution in a plane placed on the top of two DRs .	40
3.5	Realized prototype of cross-shaped DRA	42
3.6	Simulated and measured reflection coefficient	42
3.7	Simulated and measured axial ratio for the cross-shaped CP DRA	43
3.8	Simulated and measured radiation patterns at left, centre, and right of	
	the CP band	44
3.9	Simulated and measured RHCP gain	45
3.10	Sketch of the improved antenna design	46
3.11	Simulated reflection coefficient of the improved design	47
3.12	Simulated axial ratio of the improved design	48
3.13	Simulated radiation pattern of the improved design	48
3.14	Simulated useable CP angle of the initial and improved design at the centre of the AR bandwidth	49
4.1	E-field distribution in one arm of the cross-shaped DR	53
4.2	Realized prototype of the dual-port cross-shaped DRA	54
4.3	Top, bottom, ground plane, and side view of the cross-shaped DRA us-	
	ing one-side feeding	55
4.4	Simulated S parameters of the cross-shaped DR using one-side feeding .	56
4.5	Side view of the proposed multifunction cross-shaped DRA	56
4.6	Simulated E-field distribution of ${\rm TE}_{111}$ and Quasi- ${\rm TM}_{111}$ mode at 4.7 GHz	
	in one rectangular arm of the cross-shaped DR using one-side feeding lines	57
4.7	Simulated E-field distribution of TE_{111} and Quasi- TM_{111} mode at 4.7 GHz	
	in one parallelogrammatic arm of the cross-shaped DR using one-side	- 0
	feeding lines	58
4.8	Simulated S parameters of the cross-shaped DR composed by two parallelogrammatic arms using one-side feeding	58
4.9	Simulated E-field distribution of TE_{111} and Quasi- TM_{111} mode at 4.7 GHz	
1.,	in one rectangular arm of the cross-shaped DR using two-side feeding .	59
4.10	Simulated S parameters of the cross-shaped DR using two side feeding .	59
4.11	Top, side and bottom view of the feeding network for the proposed an-	
	tenna	60

4.12	Simulated S parameters of different values of centre probe diameter	61
4.13	Simulated S parameters of different values of centre probe height	61
4.14	Simulated E-field distribution of Quasi- TM_{111} mode in one rectangular arm of the cross-shaped DR using two-side feeding	62
4.15	Simulated and measured antenna reflection and coupling coefficient for Port 1 (TE_{111} mode) and Port 2 (Quasi- TM_{111} mode)	63
4.16	Simulated and measured axial ratio of Port 1	64
4.17	Simulated and measured circularly polarized radiation patterns of Port 1 at 4.52, 4.70 and 4.84 GHz	65
4.18	Simulated and measured linearly polarized radiation patterns of Port 2 at 4.52, 4.70 and 4.84 GHz	66
4.19	Simulated and measured linearly polarized radiation patterns of Port 2	
	at 5.5 and 6 GHz	67
4.20	Simulated and measured gain of Port 1 and 2	68
4.21	Simulated 3D radiation patterns at 4.93 and 5.54 GHz	68
4.22	Simulated and measured mean effective gain	70
4.23	Simulated and measured ratio of mean effective gain of Port 1 and 2	70
4.24	Simulated and measured envelope correlation coefficients	73
5.1	(a). Field distribution of $\text{TE}_{01\delta}$ mode in a cylindrical DR. (b). A balanced coupling method by placing two arc-shaped microstrip feeding lines in	
	each side of a DR	78
5.2	Simulated reflection coefficient for two DRAs, showing the increase of bandwidth resulting from the addition of a 1 mm air gap	79
5.3	Side and top view of the proposed antenna	80
5.4	Simulated reflection coefficient of different the lower cylinder height and radius values	81
5.5	Top view of electric field distribution inside the DR with 1 mm air gap .	81
5.6	Side view (YZ plane) of magnetic field distribution inside the DR with	
	1 mm air gap	82
5.7	Simulated 3D radiation patterns of the $TE_{01\delta}$ mode at 3.9 GHz and the $HEM_{21\delta}$ mode at 5.1 GHz	82
5.8	Simulated impedance bandwidth for different values of α	83
J.J	2	

5.9	Simulated radiation patterns at the upper limit of the bandwidth, for	
	different values of α	84
5.10	Realized prototype of horizontally polarized DRA	85
5.11	Simulated and measured antenna reflection coefficient	85
5.12	Bottom view of the substrate showing the ground plane	86
5.13	Simulated and measured gain patterns at 3.9 GHz	87
5.14	Simulated and measured maximum gain of the conical pattern	87
6.1	Prototype of the proposed dual polarized omnidirectional DRA with	
	schematic field distributions for the two orthogonal modes excited	91
6.2	Geometry of the proposed dual-polarized DRA	93
6.3	Prototype of DR	94
6.4	Simulated reflection coefficient and impedance of Port 1	95
6.5	Simulated reflection coefficient of Port 1 with different length of $L_1 \ldots$	96
6.6	Simulated reflection coefficient of Port 1	96
6.7	Physical layout of the substrate	96
6.8	Top (a) and bottom (b) view of the first prototype antenna without back	
	cavity	97
6.9	Simulated radiation patterns of Port 2 of the first prototype antenna	
	without back cavity	97
6.10	The realized feeding network	98
6.11	The comparison between the calculated resonance frequency of $\text{TE}_{01\delta}$ and $\text{TM}_{01\delta}$ mode in a cylindrical DR with dielectric permittivity of 10	99
6.12	Simulated reflection coefficient of Port 2 for different values of inner ra-	
	dius of the annular cylindrical DR	99
6.13	Simulated and measured magnitude of the antenna reflection coefficient	
	for both ports (a) and inter-port coupling coefficient (b) $\dots \dots$	100
6.14	Simulated and measured radiation pattern of Port 1 (HP) at 3.93 GHz	101
6.15	Simulated and measured radiation pattern of Port 2 (VP) at 3.93 GHz	102
6.16	Simulated and measured maximum gain of the conical pattern of Port 1	
	and 2	102
6.17	Simulated and measured envelope correlation coefficients and mean ef-	
	fective gain	103

7.1	effect model
7.2	Calculated complex permittivity of silver using the Drude model 110
7.3	3D sketch of the proposed scalable DRA model
7.4	3D HFSS model of the proposed scalable DRA model
7.5	Field distribution in the cylindrical DR mounted on a PEC block 113
7.6	Scaling behaviour of a cylindrical DRA from microwave to visible fre-
	quencies
7.7	Mesh plot of DRAs simulated in HFSS
7.8	Number of generated tetrahedra for the resonant DRA models at differ-
	ent frequencies
7.9	The cross section view of the E field amplitude and mesh
7.10	Magnitude and phase of the Y-component direction magnetic field at the probe location
7.11	Field distributions in the cylindrical DR and silver excited by a wave-
	length of 500 THz incident plane wave
8.1	3D HFSS model of the TiO ₂ -Silver DR array model
8.2	Phase and magnitude variation of DR diameter with different distance
	between DR centre at 474 THz
8.3	Phase and magnitude variation of DR diameter with different DR height at 474 THz
8.4	Partial view of 6-element DRA reflectarray
8.5	Numerically resolved phase and magnitude response of DRs with height
0.0	of 50 nm at 474 THz
8.6	Numerically resolved phase and magnitude response of DRs with and
	without silicon layer at 474 THz
8.7	Incident (a) and scattered (b) electric fields of 6-element subarray DRA
	reflectarray for the TE polarized wave
8.8	Incident (a) and scattered (b) electric fields of 6-element subarray DRA
	reflectarray for the TM polarized wave
8.9	Scattered electric fields of 4 element DRA reflectarray for the TE (a) and
	TM (b) polarized normal incident wave

8.10	Scattered electric fields of 9 element DRA reflectarray for the TE (a) and
	TM (b) polarized normal incident wave
8.11	Schematic of the fabrication sequence for the optical DRA reflectarray . 132
8.12	(a) Photo of fabricated DRA reflectarrays; (b) Zoomed in picture of 4
	areas with the same reflectarray layout. (c) Zoomed in picture of one area 132
8.13	Scanning electron micrograph revealing an area on the fabricated 4, 6
	and 9-element reflectarrays
8.14	Designed and realized DR diameters of 4, 6 and 9-element reflectarrays . 134
8.15	Experiment setup
8.16	Beam reflection patterns obtained from a CCD camera
8.17	3D representation of the beam shapes for the 6-element reflectarray mea-
	sured by the Thorlabs LC100 CCD linear camera
8.18	Normalized radiation pattern of 6 element reflectarray
8.19	Normalized beam reflection pattern of 6 element reflectarray 137
8.20	Numerically resolved phase and magnitude response of DRs by using
	different silver permittivity at 474 THz
8.21	Scanning electron micrograph revealing an area on the fabricated 6 and
	9 element reflectarrays
8.22	Designed and realized DR diameters of 6 and 9 element reflectarray 140
8.23	CCD imaging of beam reflection patterns excited by TE polarized inci-
	dent wave
8.24	The beam reflection patterns obtained from array theory calculation (a),
	the linear camera (b) and CCD camera (c)
8.25	Measured radiation pattern of 6 element reflectarray in the second sample 141
8.26	Numerically resolved phase and magnitude response of of silver and
	uniform DRA array with different dielectric loss tangent at 474 THz 142
8.27	Scanning electron micrograph revealing an area on the fabricated uni-
	form DRA array
8.28	Reflection power from uniform array measurement
8.29	Grating reflector with the same TiO_2 volume as DRA reflectarray 144
8.30	Scattered electric fields of grating reflector for the TE (a) and TM (b)
	normally polarized incident waves

List of Tables

3.1	Antenna parameters of the CP DRA	41
3.2	Antenna parameters of the improved CP DRA	46
4.1	Antenna parameters of the Multifunction and diversity DRA	60
5.1	Antenna parameters for the final design, in the geometry of Fig. 5.3	83
5.2	Comparison between horizontally-polarized omnidirectional antennas .	88
6.1	Antenna parameters of the dual polarized DRA	92
8.1	DR diameters of 6-element subarray. The calculated angle of deflection	
	is 17.5°	127
8.2	DR diameters of 4-element subarray. The calculated angle of deflection	
	is 27.0°	130
8.3	DR diameters of 9-element subarray. The calculated angle of deflection	
	is 11.6°	130